

# Synthesis and Evaluation of Maleic Anhydride-Methyl Oleate Copolymer as a Corrosion Inhibitor for C-steel in 0.1 M HCl Solution

R.J. Tuama<sup>1</sup>, M.E. Al-Dokheily<sup>2,\*</sup> and M.N. Khalaf<sup>3</sup>

<sup>1</sup> Department of Pharmacognosy, College of Pharmacy, Thi-Qar University, Iraq

<sup>2</sup> Department of Chemistry, College of Science, Thi-Qar University, Iraq

<sup>3</sup> Department of Chemistry, College of Science, Basrah University, Iraq

\*E-mail: [mohsin552015@gmail.com](mailto:mohsin552015@gmail.com)

Received: 3 August 2020 / Accepted: 26 September 2020 / Published: 31 October 2020

---

The present study investigated the synthesis of a copolymer of maleic anhydride and an ester of oleic acid. Poly (maleic anhydride-co-methyl oleate) was prepared via the free radical polymerization of maleic anhydride with methyl oleate. The prepared copolymer was characterized via FTIR and GPC and thermal analyses (TGA and DTA). TGA demonstrated that the prepared copolymer was thermally stable up to 146 °C. Electrochemical measurement tests, including potentiodynamic polarization tests, revealed that the prepared copolymer was successfully applied as an organic corrosion inhibitor for C-steel in 0.1 M HCl solution at 298 K, 308 K, 318 K and 328 K. Potentiodynamic polarization measurements revealed that this copolymer was a mixed-type corrosion inhibitor. Its inhibition efficiency was measured on the basis of potentiodynamic polarization curves via the electrochemical technique. Results demonstrated that the corrosion inhibition efficiency of poly(maleic anhydride-co-methyl oleate) increased with concentration and decreased with increasing temperature. Inhibition efficiency reached 94.8% with 20 ppm poly (maleic anhydride-co-methyl oleate) at 298 K. The adsorption of this copolymer on the C-steel surface was chemical adsorption and obeyed the Langmuir adsorption isotherm.

---

**Keywords:** copolymer, free radical polymerization, organic corrosion inhibitor, potentiodynamic polarization, Langmuir adsorption isotherm.

## 1. INTRODUCTION

Corrosion is one of the intractable problems faced by industrial progress. Therefore, corrosion has been called industrial cancer, and its resulting material losses are exorbitant and important due its numerous related variable factors [1, 2]. The internal corrosion of carbon steel pipelines designed for long-term operation is a common and serious problem in oil and gas production. It involves an interaction between metal walls and flowing fluids. This problem has resulted in the consideration of many

corrosion control programs and research in various oilfields around the world [3]. Organic compounds containing N, S and O heteroatoms in their structures and pi-electron systems are commonly used as inhibitors to protect metals from corrosion in numerous aggressively acidic media. The efficiency of these compounds mainly relies on their capabilities for adsorption on metal surfaces with their polar groups acting as reactive centers [4-7]. In recent years, organic polymers have attracted considerable attention in studies on corrosion inhibition because many of them exhibit the characteristics of high safety, nontoxicity, inherent stability, cost-effectiveness and high inhibition efficiency at considerably low concentrations [8,9]. Polymers tend to form complexes with metal ions and adsorb on metallic surfaces effectively due to the presence of various functional groups. Polymer molecules or their metal complexes occupy a large surface area, thereby blanketing surfaces and protecting the metal from the corrosive agents present in the solution [10, 11]. The inhibitive strength of these polymers is connected basically to cyclic rings and heteroatoms (S, O or N) that are the major active centers of adsorption. These materials need not be very high in molecular weight and are often oligomeric with less than 10 repeat units being sufficient for their desired function. Polymers have the upsides of better film-forming capabilities, multifunctionality, flexible viscosity, solubility and higher number of attachment points to metal surfaces over widely used small-molecule corrosion inhibitors [12].

Various studies have introduced polymers as good coating materials and corrosion inhibitors. Sudershan et al. utilized polyurethane-based triblock copolymers as inhibitors for corrosion on mild steel in 0.5 M H<sub>2</sub>SO<sub>4</sub> solution. These copolymers were synthesized through the atom transfer radical polymerization mechanism. The corrosion inhibition effectiveness of polymers has been explored by using electrochemical measurements, surface analysis, quantum chemical calculations and molecular dynamic simulations. The results of previous investigations demonstrated that the inhibitive effects of the polymers increase with increasing concentration and decrease with increasing temperature. The adsorption behaviour of these polymers on the MS surface obeys the Langmuir adsorption isotherm and involves physisorption and chemisorption mechanisms [13]. Al Juhaiman studied the utilization of polyvinyl pyrrolidone (PVP) as a corrosion inhibitor for C-steel in 2 M HCl. The inhibitory impact of the green inhibitor PVP on the corrosion of C-steel in aerated, unstirred 2 M HCl solutions were examined over a range of concentrations and temperatures by using electrochemical (electrochemical impedance spectroscopy [EIS] and Potential dynamic polarization) and gravimetric methods. Tafel results showed that PVP was a mixed-type inhibitor that affected iron dissolution and hydrogen evolution. The adsorption of PVP on the C-steel surface obeyed the Langmuir adsorption isotherm. The inhibition efficiency of PVP increased with increasing inhibitor concentration and increasing temperature [14]. Tsoeunyane et al. synthesized polybutylene succinate extended with 1,6-diisocynato-hexane-L-histidine composite (PBSLH) via condensation polymerization. The use of the synthesized composite as corrosion inhibitor for mild steel in 1 M HCl was investigated on the basis of conventional weight loss, potentiodynamic polarization, variable amplitude sinusoidal micropolarization (VASP) and EIS analyses. The maximum inhibition efficiency was achieved at 78% at a concentration of 600 ppm. The adsorption of PBSLH followed the Langmuir model, and PBSLH was identified as mixed-type corrosion inhibitor [15].

In the present work, poly(maleic anhydride-co-methyl oleate) was synthesized. Its corrosion inhibition performances on C-steel in 0.1 M HCl was characterized and tested.

## 2. EXPERIMENTAL

### 2.1. Materials

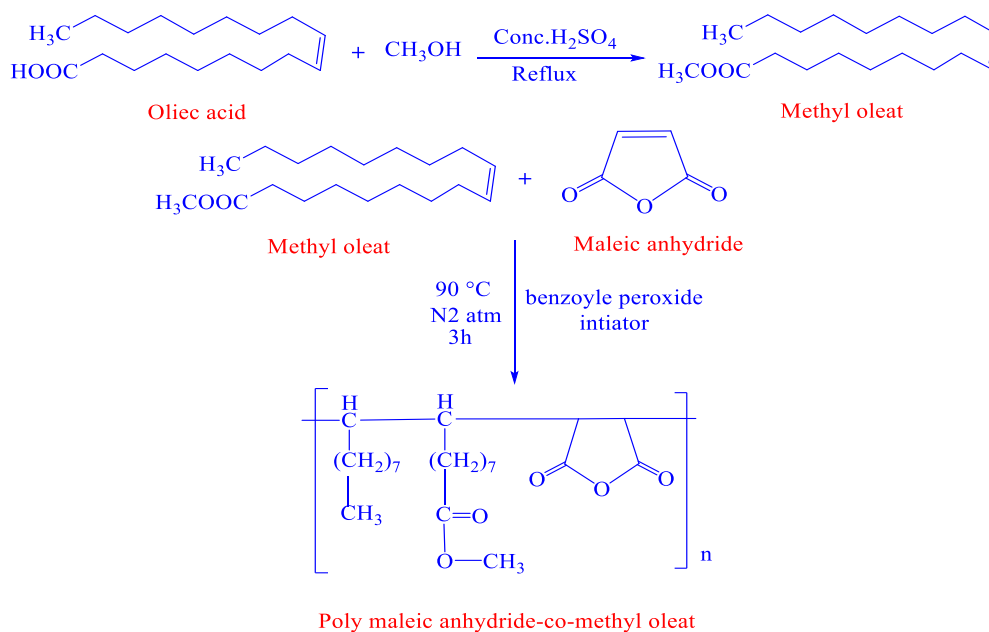
Carbon steel (C1010) was purchased from Alabama Company (U.S.A). Its composition by percentage weight was as follows: C = 0.13%, Mn = 0.3%, Si = 0.37%, P = 0.04%, S = 0.05%, Cr = 0.1%, Ni = 0.3%, Cu = 0.3% and As = 0.08%. Fe was balanced. Maleic anhydride, oleic acid, methanol alcohol, anhydrous sodium sulphate, benzoyl peroxide and toluene were purchased from Sigma-Aldrich/Germany. Hydrochloric acid and sulphuric acid were purchased from BDH/England.

### 2.2. Synthesis of poly(maleic anhydride-co-methyl oleate)

#### a- Esterification of oleic acid

In a 100 mL round-bottomed flask with a reflux condenser, oleic acid (16.75 mL, 0.05 mol) was esterified with an excess of methanol alcohol with concentrated sulphuric acid as a catalyst. The reaction mixture was heated at 69 °C by utilizing a Hongsonic Ultrasonic Bath (HS-100) from China for 2 h. After esterification was finished, the product was put into a separating funnel for 1 h to obtain two separate layers. The bottom layer of the unreacted materials and water was removed and collected, and the top layer, namely, the organic layer, was separated and dried over anhydrous Na<sub>2</sub>SO<sub>4</sub>. The prepared ester was subjected to the saponification method [16].

#### b- Copolymerization



**Scheme 1.** Preparation of poly(maleic anhydride-co-methyl oleate)

The prepared methyl oleate was copolymerized with maleic anhydride at a 1:2 molar ratio via free radical polymerization. Polymerization was conducted under nitrogen atmosphere by using benzoyl peroxide as an initiator (2% w/w) dissolved in 20 mL of toluene. The initiator was added gradually to

the reaction mixture at 90 °C for 3 h with constant stirring. The copolymer product was dried under vacuum for 24 h [17, 18]. The synthesis of poly (maleic anhydride-co-methyl oleate) is shown in Scheme 1.

### 2.3. Characterization of the synthesized copolymer

A Bruker–Vertex FTIR spectrophotometer was utilized to reveal the chemical structure of the synthesized copolymer on the basis of Fourier transform infrared spectral data obtained over the 400–4000  $\text{cm}^{-1}$  wavenumber range. The number average molecular weight ( $M_n$ ) of this copolymer was determined by gel permeation chromatography (GPC) with a refractive index detector by using Breeze™ 2 HPLC System. THF (Merck) was utilized as the eluent at a flow rate of 1.0 mL/min. Bahr-Thermo analyser (STA 503) was applied for the thermal analysis study (TGA and DTA). The rate of heating was 20 °C /min in an inert argon atmosphere.

### 2.4. Corrosion inhibition measurements

Corrosion inhibition measurements were performed by using a DY 2300 Series Potentiostat/Bipotentiostat that was fully computerized for the analysis of processed data. The potential range was init. E(V)-0.203 to end E(V)-1.203 , and the scan rate was 2.5 mV/sec . A three-electrode cell assembly consisting of C-steel as the working electrode, platinum as the counter electrode and a silver–silver chloride electrode as the reference electrode was used. Carbon steel was immersed in acidic solution containing 0.1 M HCl with various concentrations (5, 10, 15, 20 and 25 ppm) of poly(maleic anhydride-co-methyl oleate) as the corrosion inhibitor at different temperatures (298 K–328 K). A water bath was used to maintain the temperature at the required temperature of the electrolyte. From the polarization data, the following parameters were obtained: inhibition efficiency percentage (%IE), degree of surface coverage ( $\theta$ ) and corrosion rate (CR) [14,19]. The effectiveness of inhibition was determined by using Equation (1), whereas  $\theta$  was determined by using Equation (2).  $CR_{(\text{uninhib})}$  and  $CR_{(\text{inhib})}$  are the values of the CR of C-steel in the absence or presence of the inhibitor, respectively [20, 21].

$$\%IE = \frac{CR_{\text{uninhib}} - CR_{\text{inhib}}}{CR_{\text{uninhib}}} \times 100 \quad (1)$$

$$\theta = \frac{CR_{\text{uninhib}} - CR_{\text{inhib}}}{CR_{\text{uninhib}}} \quad (2)$$

## 3. RESULTS AND DISCUSSION

### 3.1. Characterization of the synthesized copolymer

Figure 1 shows the FTIR spectrum of poly(maleic anhydride-co-methyl oleate). The peaks at 2924.09 and 2854.65  $\text{cm}^{-1}$  for the asymmetric and symmetric stretching vibration of C-H. The FTIR

spectrum of this copolymer shows two absorption bands containing a relatively intense absorption band at  $1782.23\text{ cm}^{-1}$  and a weak one at near  $1851.66\text{ cm}^{-1}$ , which are ascribed to C=O group stretching of the saturated cyclic anhydride ring due to the symmetric and asymmetric C=O stretching respectively [22,23], while the strong absorption band which appears at  $1743.65\text{ cm}^{-1}$  is assigned to C=O group stretching of ester. The presence of absorption bands in the range  $1300\text{-}900\text{ cm}^{-1}$  refer to stretching vibration of C-O bonds of maleic anhydride and ester.

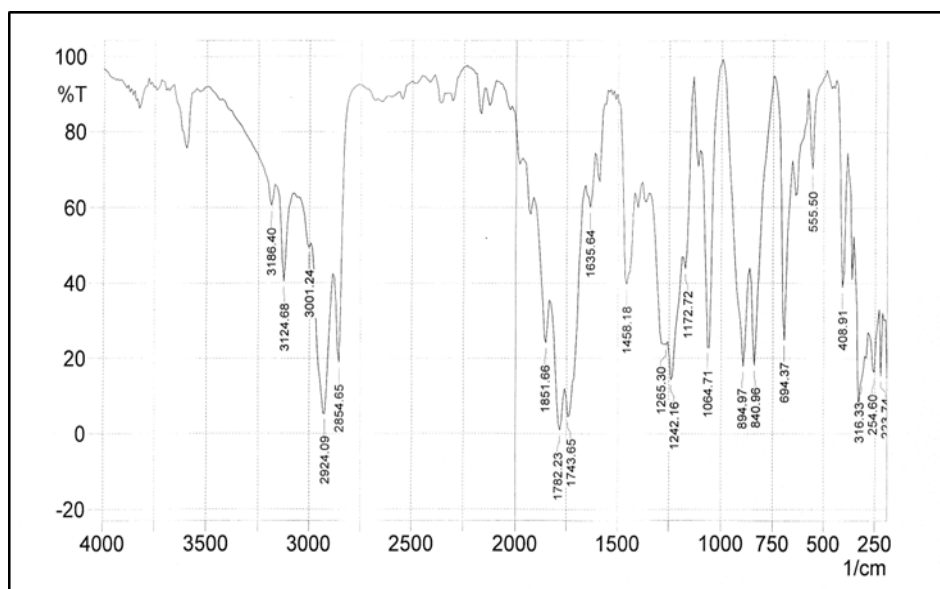


Figure 1. FTIR spectrum of poly (maleic anhydride-co-methyl oleate)

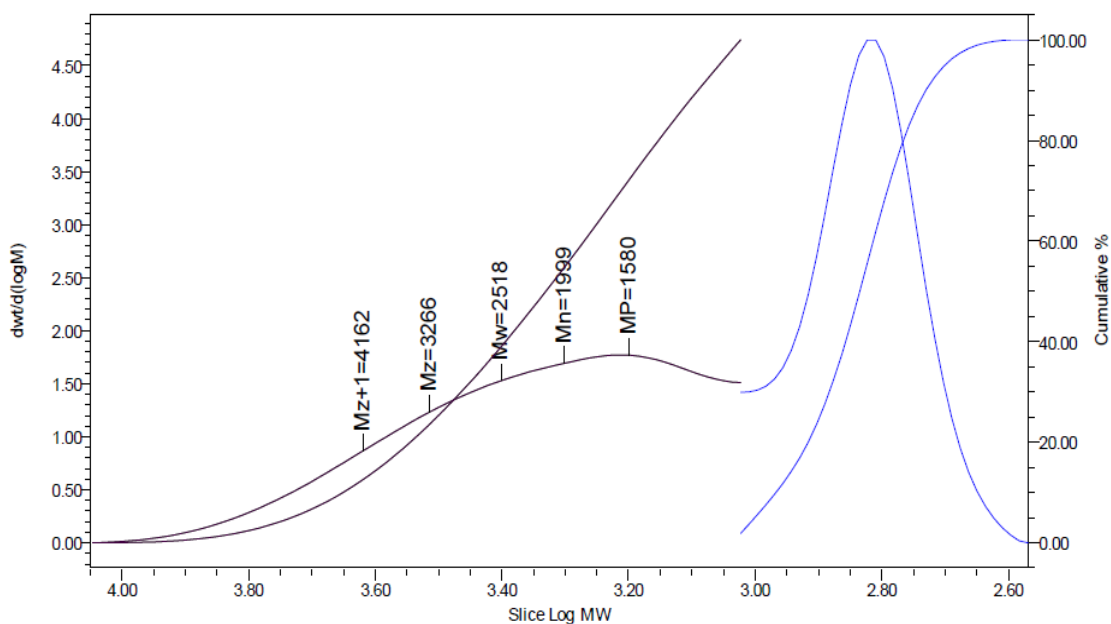


Figure 2. GPC chromatograms of poly (maleic anhydride-co-methyl oleate)

Figure 2 shows the GPC of the copolymer, and Table 1 provides the number-average molecular weight ( $M_n$ ), the weight-average molecular weight ( $M_w$ ) and the peak molecular weight ( $M_p$ ) of poly(maleic anhydride-co-methyl oleate). The polydispersity index ( $M_w/M_n$ ) was equal to (1.259), indicating that polymerization was good and that the number of chains was not excessive.

**Table 1.** Molecular weights of poly (maleic anhydride-co-methyl oleate)

$M_n$	$M_w$	$M_p$	$M_w/M_n$
1999	2518	1580	1.259

### 3.2. Electrochemical measurements

#### 3.2.1. Potentiodynamic polarization measurements

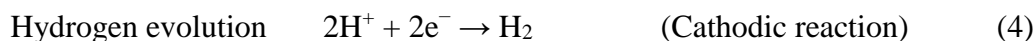
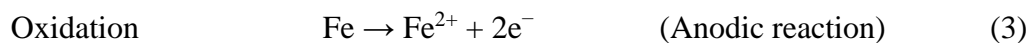
The respective potentiodynamic polarization parameters, inhibition efficiency (%IE), surface coverage ( $\theta$ ) and corrosion rate (CR) in presence and absence of different concentrations of poly(maleic anhydride-co-methyl oleate) at various temperatures (298 K–328 K) are shown in Table 2. potentiodynamic polarization curves in the presence and absence of different concentrations of this copolymer at various temperatures are provided in Figures 3-5.

**Table 2.** Electrochemical data for C-steel in 0.1 M HCl in the absence and presence of different concentrations of synthesized copolymer at different temperatures

conc. (ppm)	$T$ (K)	$E_{corr}$ (mV)	$Ba$ (mV. dec <sup>-1</sup> )	$Bc$ (mV. dec <sup>-1</sup> )	$I_{corr}$ ( $\mu$ A/cm <sup>2</sup> )	CR (mpy)	%IE	$\theta$
Blank		-617	233	-241	1056	116	-	-
5	<b>298</b>	-681	246	-251	195.360	21.46	81	0.81
10		-653	256	-258	163.891	18.00	84	0.84
15		-604	259	-267	104.544	11.40	90	0.90
20		-537	245	-263	54.912	6.00	94	0.94
25		-495	263	-265	64.732	7.10	93	0.93
Blank			-611	250	-249	1120	128	-
5	<b>308</b>	-663	262	-266	210.000	24.00	81	0.81
10		-631	252	-251	200.480	22.80	82	0.82
15		-560	250	-248	122.528	14.00	89	0.89
20		-600	246	-245	87.584	10.00	92	0.92
25		-575	249	-240	89.264	10.20	92	0.92
Blank			-625	238	-257	1304	183.6	-

5	-624	240	-251	263.538	37.10	79	0.79
10	-622	239	-256	260.669	36.70	80	0.80
15	-615	236	-259	155.697	22.00	88	0.88
20	-607	239	-261	121.272	17.00	90	0.90
25	-611	241	-262	127.922	18.00	90	0.90
Blank	-628	246	-282	1430	259	-	-
5	-665	248	-283	320.892	58.10	77	0.77
10	<b>328</b>	251	-289	304.590	55.00	78	0.78
15	-679	252	-284	233.090	42.00	83	0.83
20	-602	250	-281	177.320	32.00	87	0.87
25	-610	248	-284	182.325	33.00	87	0.87

As shown in Table 2, the addition of 5-20 ppm poly(maleic anhydride-co-methyl oleate) inhibitor at different temperatures decreased corrosion current density ( $I_{corr}$ ) and CR. By contrast, %IE increased as the inhibitor concentration was increased. These results indicated that the amount of inhibitor molecules adsorbed on the surface of C-steel working electrode was positively correlated with its concentration. The corrosion inhibitor film could effectively prevent corrosive ions from directly contacting the working electrode, and the degree of corrosion of C-steel decreased [24]. When the concentration of poly (maleic anhydride-co-methyl oleate) inhibitor exceeded 20 ppm,  $I_{corr}$  was positively proportional to the concentration value, and %IE was inversely proportional to the concentration value. This relationship might indicate that when the added amount of this inhibitor exceeded a maximum value, a mutual repulsion effect occurred between inhibitor molecules, resulting in the weakening of the corrosion inhibitor film and a decrease in %IE [25]. The  $E_{corr}$  of the working electrode in the corrosion inhibition system was less than 85 mV; thus, the poly(maleic anhydride-co-methyl oleate) inhibitor was a mixed-type corrosion inhibitor [26,27]. Furthermore, the  $\beta_a$  and  $\beta_c$  values in Table 2 were unstable, indicating that corrosion was inhibited but that the mechanism of anodic dissolution of the alloy and hydrogen evolution was uncontrolled and inhibition was achieved via simple blocking reaction [28,29]. The cathodic and anodic reactions are represented by the following equations:



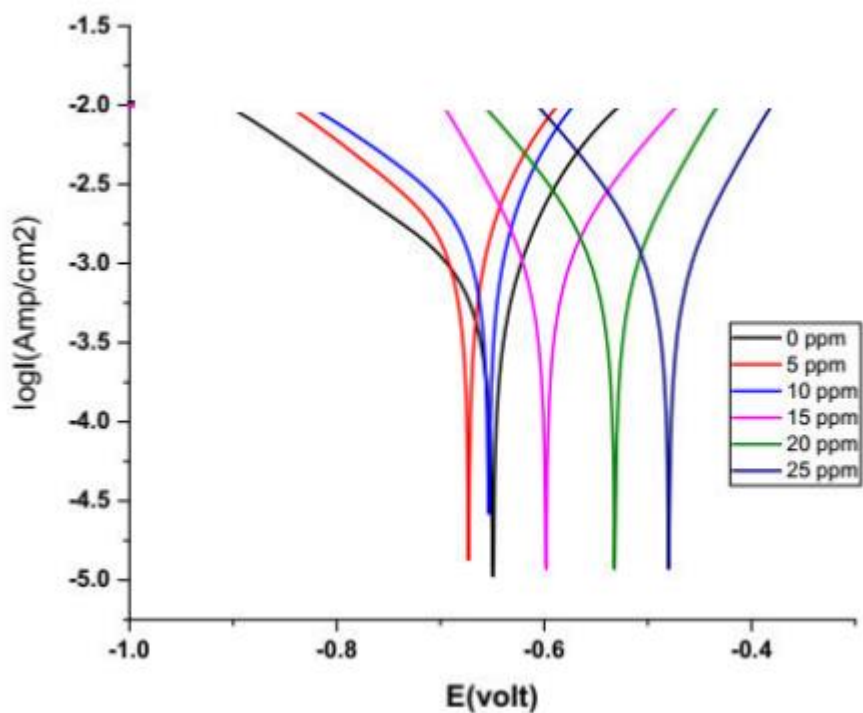


**Figure 3.** Potentiodynamic polarization curves for C-steel in 0.1 M HCl in the absence and presence of various concentrations of synthesized copolymer at 298 K.

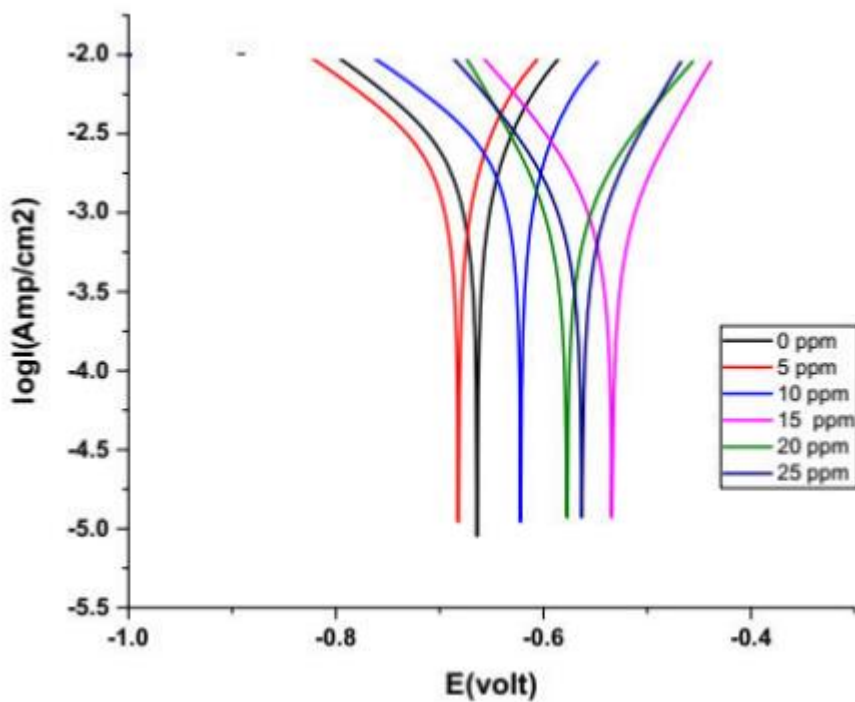


**Figure 4.** Potentiodynamic polarization curves for C-steel in 0.1 M HCl in the absence and presence of various concentrations of synthesized copolymer at 308K.



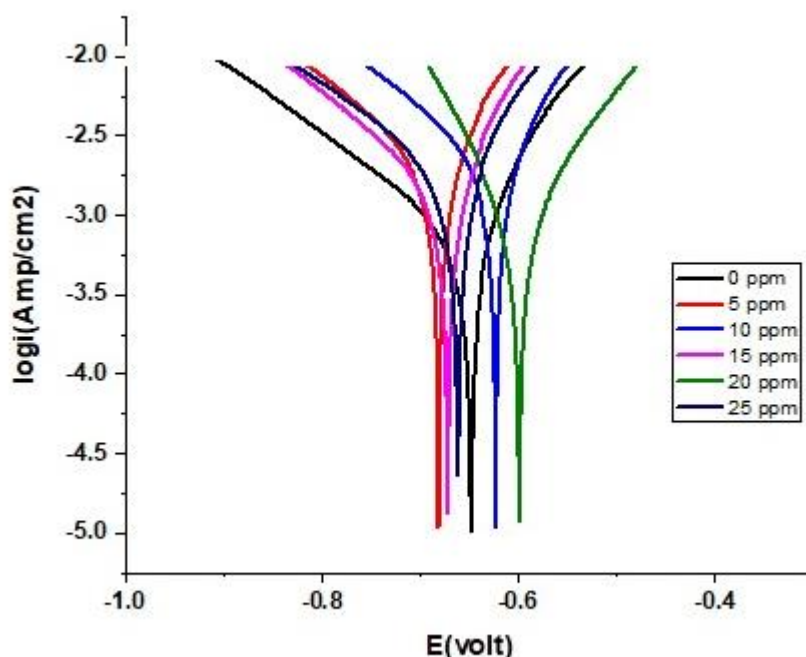


**Figure 5.** Potentiodynamic polarization curves for C-steel in 0.1 M HCl in the absence and presence of various concentrations of synthesized copolymer at 328K

3.2.2. Effect of temperature on corrosion

The influence of increasing temperatures from 298 K to 328 K on the CR of C-steel in 0.1 M HCl and %IE at different concentrations of poly(maleic anhydride-co-methyl oleate) are shown in Tables 3 and 4, respectively. CR increased with the increase in temperature as a result of the increase in the average kinetic energy of the reacting molecules.

**Table 3.** Effect of temperature on the CR of C-steel in the absence and presence of various concentrations of the inhibitor copolymer.

T(K)	Corrosion Rate (mpy)				
	5 ppm	10 ppm	15 ppm	20 ppm	25 ppm
298	21.46	18	11.4	6	7.1
308	24	22.8	14	10	10.2
318	37.1	36.7	22	17	18
328	58.1	55	42	32	33

Table 4 shows that that the %IE of various concentrations of the inhibitor copolymer decreased with the increase in temperature because increasing the temperature increased the kinetic energy and

diffusion of inhibitory particles, as well as reduced corrosion potential. Thus, adsorption efficiency and the surface area covered by the particles decreased, or the formed layer was heterogeneous and light.

**Table 4.** Effect of temperature on the %IE of the inhibitor at different concentrations of the copolymer inhibitor

<i>T(K)</i>	%IE				
	5 ppm	10 ppm	15 ppm	20 ppm	25 ppm
298	81.5	84.48	90.1	<b>94.8</b>	93.87
308	81.25	82.1	89.06	92.18	92.03
318	79.79	80.01	88.06	90.7	90.19
328	77.56	78.7	83.7	87.6	87.25

### 3.2.3 Thermodynamic parameters

The kinetic of corrosion reaction was studied in the absence and the presence of the inhibitor copolymer, where the activation energy  $E_a^*$  and thermodynamic functions of activations like activated enthalpy  $\Delta H_a^*$ , and activated entropy  $\Delta S_a^*$  were calculated from Arrhenius equation and its alternative formulation called transition state equation according to the following equations [30]:

$$CR = A \exp\left(-\frac{E_a^*}{RT}\right) \quad (5)$$

$$CR = \frac{RT}{Nh} \exp\left(\frac{\Delta S_a^*}{R}\right) \exp\left(-\frac{\Delta H_a^*}{RT}\right) \quad (6)$$

where CR is the corrosion rate, A is the pre-exponential factor,  $E_a^*$  is the activation energy, h is Planck's constant ( $6.626176 \times 10^{-34}$  J·s), N is Avogadro's number ( $6.02252 \times 10^{23}$  mol<sup>-1</sup>), R is the universal gas constant, T is the absolute temperature,  $\Delta H_a^*$  is the enthalpy of activation and  $\Delta S_a^*$  is the entropy of activation. Generally, the activation energy of corrosion in the presence of poly (maleic anhydride-co-methyl oleate) was greater than that in a corrosive environment, where the inhibitor reduced CR by preventing the corrosive ions of HCl from adsorbing on the surfaces of the alloy and decreasing the capability of the inhibitor to attenuate the corrosion reaction [31].

As shown in Figure 6, the value of  $E_a^*$  could be obtained from the slope ( $-E_a^*/R$ ) of the straight line (Table 5) in the Arrhenius plots of Log CR versus 1/T of C-steel for blank solution and different concentrations of poly(maleic anhydride-co-methyl oleate).  $E_a^*$  values increased with the increase in the concentration of poly(maleic anhydride-co-methyl oleate) and were higher than those in the absence of the inhibitor, wherein the dissolution of C-steel was decreased due to the formation of the high-energy barrier by the adsorption of the inhibitor copolymer on the metal surface, indicating that the adsorption of the inhibitor was facilitated as the inhibitor concentration was increased [32, 33].

The thermodynamic functions of activation for C-steel corrosion in 0.1 N HCl in the absence and presence of different concentrations of the copolymer inhibitor were calculated in accordance with Equation (6) by plotting  $\log(CR/T)$  as a function of  $1/T$  (Figure 7), wherein the slope was  $(-\Delta H_a^*/2.303 R)$  and the intercept was  $(\log R/Nh + \Delta S_a^*/2.303 R)$  from which the  $\Delta H_a^*$  and  $\Delta S_a^*$  values were calculated (Table 5). The positive signs of the enthalpies  $\Delta H_a^*$  for the system indicated that C-steel dissolution was endothermic. The value of  $\Delta S_a^*$  provided in Table (5) reveals that these values increased positively in the presence of the inhibitor but not in its absence, revealing that disorder increases from the reactant to the activated complex [34].

**Table 5.** Activation energy and thermodynamic functions of activation in the absence and presence of the copolymer inhibitor at different concentrations.

<i>Inhibitor conc. (ppm)</i>	<i>E<sub>a</sub><sup>*</sup> (kJ/mol)</i>	<i>ΔH<sub>a</sub><sup>*</sup> (kJ/mol)</i>	<i>ΔS<sub>a</sub><sup>*</sup> (kJ/mol)</i>
0	22	19	-0.13973
5	27	25	-0.13633
10	30	28	-0.12618
15	35	32	-0.11625
20	45	42	-0.08798
25	41	39	-0.09736

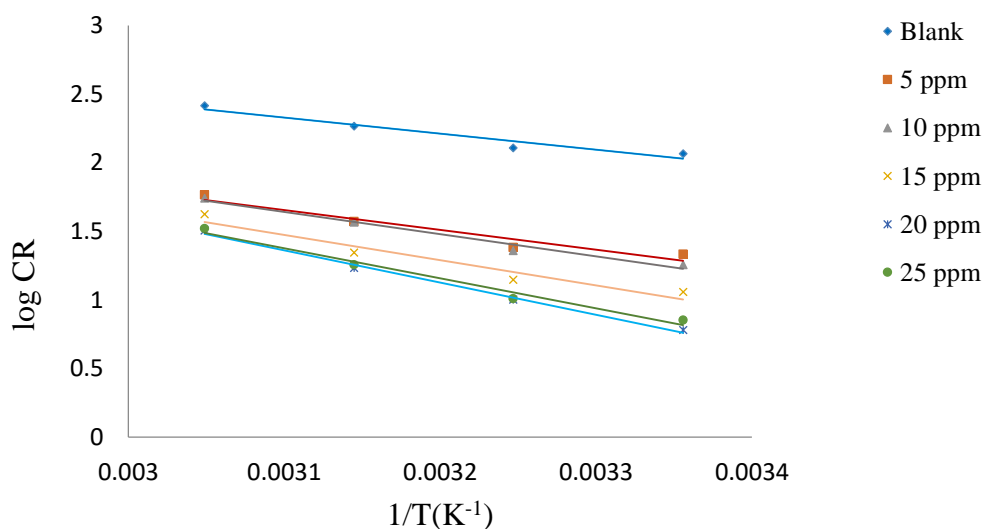


**Figure 6.** Arrhenius plots for the corrosion reaction of C-steel in the presence and absence of the inhibitor copolymer

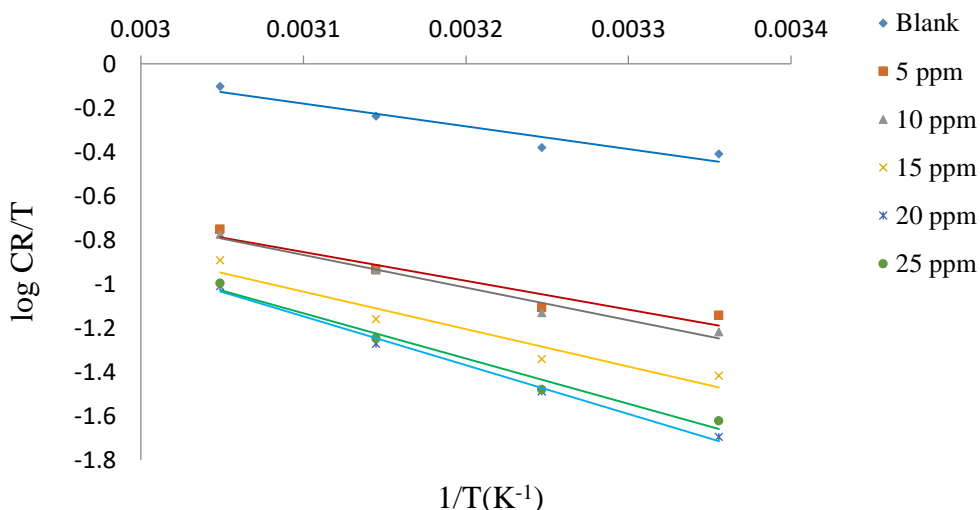


**Figure 7.** Transition state plots for the corrosion reaction of C-steel in the presence and absence of the copolymer inhibitor.

### 3.2.4. Adsorption isotherm

The adsorption isotherm provides basic information regarding the interaction between the inhibitor and the C-steel surface. In this study, the suitable adsorption isotherm for this inhibitor was the Langmuir adsorption isotherm. Although several adsorption isotherms were tested for the adsorption of the organic compound in an attempt to fit the experimental data [28, 35], only the Langmuir adsorption isotherm provided acceptable linear fits on the basis of the near-unity values of the correlation coefficient ( $R^2$ ) values. The linear form of the Langmuir adsorption isotherm is given by Equation (7) [36].

$$\frac{C}{\theta} = \frac{1}{K_{ads}} + C \tag{7}$$

where  $\theta$  is the surface coverage degree,  $C$  is the inhibitor concentration and  $K_{ads}$  is the adsorptive equilibrium constant. The Langmuir isotherms at different temperatures for different concentrations of poly (maleic anhydride-co-methyl oleate) in 0.1 M HCl are shown in Figure 8. The equilibrium constant ( $K_{ads}$ ) for the adsorption process must be calculated on the basis of the inhibitor’s Langmuir’s adsorption isotherm to calculate the thermodynamic functions of adsorption, such as the free energy of adsorption ( $\Delta G^{\circ}_{ads}$ ). Hence,  $\Delta G^{\circ}_{ads}$  can be calculated in accordance with Equation (8) as follows [37]:

$$\Delta G^{\circ}_{ads} = - RT \ln(55.5 K_{ads}) \tag{8}$$

where  $R$  is the gas constant,  $T$  is the absolute temperature and 55.5 is the molar concentration of water in aqueous solution. The values of  $K_{ads}$  and  $\Delta G^{\circ}_{ads}$  for the studied inhibitor are reported in Table 6.

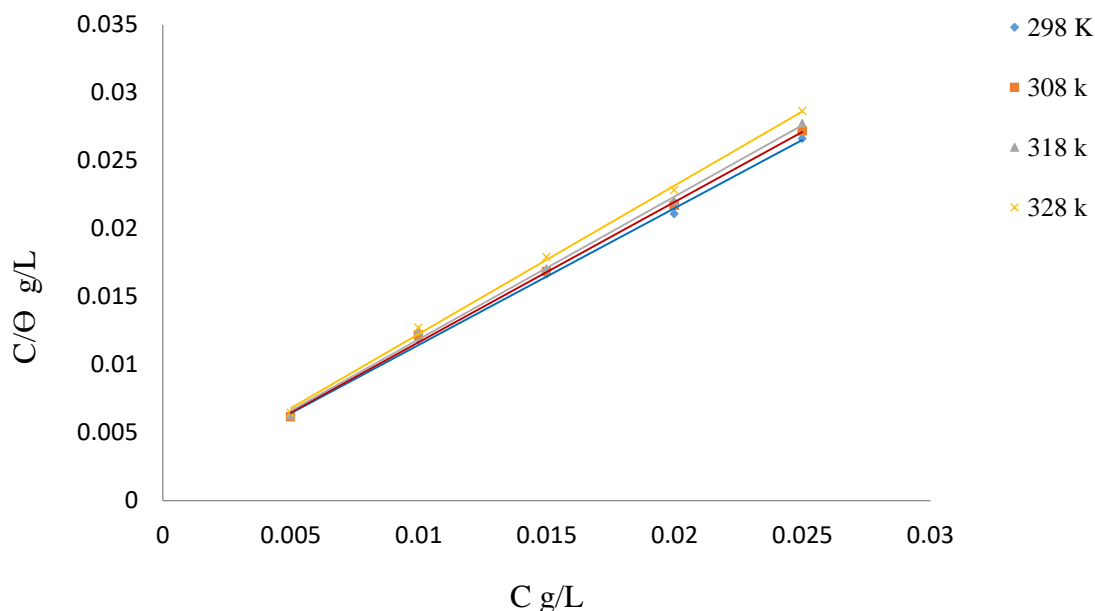


**Figure 8.** Langmuir isotherm for the adsorption of the copolymer inhibitor on the surfaces of C-steel in 0.1 M HCl.

**Table 6.** Adsorption parameters for the copolymer inhibitor on carbon steel surface in 0.1 M HCl solution at different temperatures.

<i>Inhibitor</i>	<i>T</i> (K)	<i>R</i> <sup>2</sup>	<i>K</i> <sub>ads</sub> (L·mol <sup>-1</sup> )	$\Delta G^{\circ}_{ads}$ (kJ·mol <sup>-1</sup> )
<i>Copolymer</i>	298	0.9983	714.285	-33
	308	0.9982	769.230	-34
	318	0.9977	714.285	-35
	328	0.9984	714.285	-36

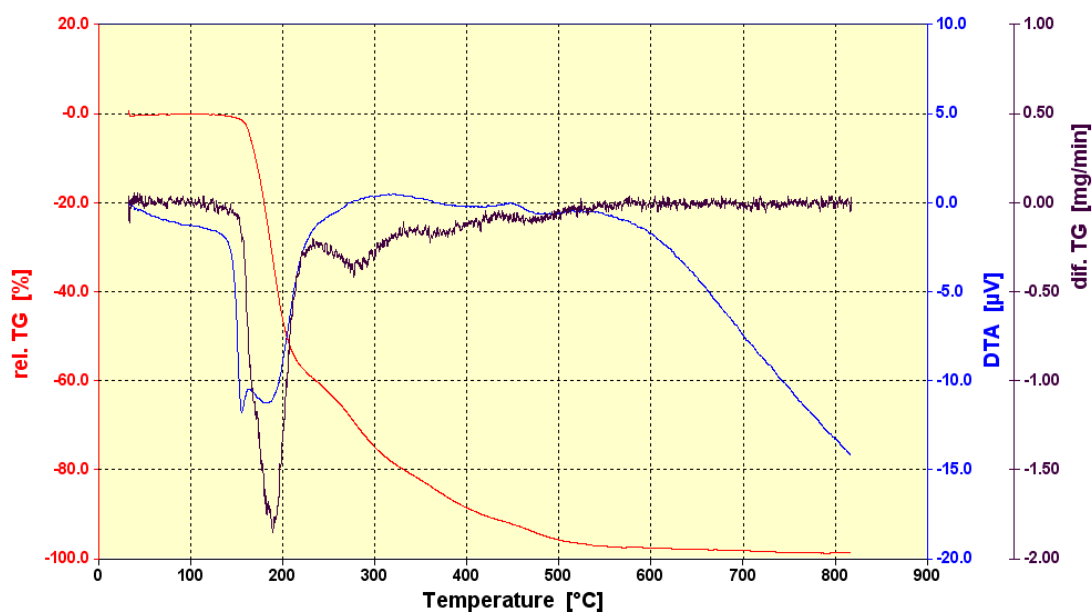
As inferred from the negative values of  $\Delta G^{\circ}_{ads}$  shown in Table (6), the adsorption of poly(maleic anhydride-co-methyl oleate) molecule on the C-steel surface was spontaneous and that a strong interaction existed between the molecules of this copolymer inhibitor and the metal surface [38-40]. The data for  $\Delta G^{\circ}_{ads}$  corresponded with the chemisorption behaviour of this inhibitor. The strong adsorption of the inhibitor molecules on the C-steel surface was due to the presence of the free electron pairs on (O) atoms. Heteroatoms, such as (O), in organic compounds act as reaction sites in adsorption [41, 42].

### 3.2.5. Thermal analysis TGA and DTA of the synthesized copolymer

TGA and DTA curves are shown in Table 7 and Figure 9. The inhibitor poly(maleic anhydride-co-methyl oleate) was thermally stable up to 146 °C. The  $T_{max}$  was 189 °C, indicating that the inhibitor was stable. The inhibitor had an initial decomposition temperature of  $T_i = 163.4$  °C and a final decomposition temperature of  $T_f = 223.6$  °C.

**Table 7.** TGA and DTA parameters of the synthesized copolymer.

Decomposition temperature ( $T_{\max}$ )	189°C
50 % wt. loss ( $T_{1/2}$ )	185°C
Char yield 15% at	361°C
$\Delta T = T_f - T_i = (223.6 - 163.4)$ °C	60.2°C

**Figure 9.** TGA and DTA curves of the synthesized copolymer

#### 4. CONCLUSION

The poly(maleic anhydride-co-methyl oleate) inhibitor prepared in this work was powerful in inhibiting the corrosion of C-steel in 0.1 M HCl. This effect was dependent on concentration and temperature. Inhibition efficiency reached 94% at 298 K with an inhibitor concentration of 20 ppm. In other words, the corrosion inhibition efficiency of this copolymer inhibitor increased with the increase in concentration and decrease in temperature. Potentiodynamic polarization measurements showed that poly(maleic anhydride-co-methyl oleate) was a mixed corrosion inhibitor. The adsorption of poly(maleic anhydride-co-methyl oleate) followed Langmuir's adsorption isotherm. The inhibitor was chemically adsorbed on the surface of C-steel. Negative  $\Delta G^{\circ}_{\text{ads}}$  values indicated that the adsorption process of this copolymer was spontaneous.

#### ACKNOWLEDGEMENT

The authors would like to express their deep gratitude to Thi-Qar University and Chemistry Department of the College of Science for supporting this work.

## References

1. N. Ahmad and A. G. MacDiarmid, *Synth. Met.*, 78 (1996) 103.
2. S. K. Shukla, M. A. Quraishi and R. Prakash, *Corros. Sci.*, 50 (2008) 2867.
3. P. R. Roberge, *Corrosion Engineering: Principles and Practice*, McGraw-Hill, (2008) New York City, USA.
4. G. Khan, K. S. Newaz, W. J. Basirun, H. B. M. Ali, F. L. Faraj and G. M. Khan, *Int. J. Electrochem. Sci.*, 10 (2015) 6120.
5. G. Sığırcık, T. Tüken and M. Erbil, *Corros. Sci.*, 102 (2016) 437.
6. A. A. Naser, A. S. Al-Mubarak and H. Z. Al-Sawaad, *Int. J. Corros. Scale Inhib.*, 8 (2019) 974.
7. H. Keleş, D. M. Emir and M. A. Keleş, *Corros. Sci.*, 101 (2015) 19.
8. B. Ramagathan, M. Gopiraman, L. O. Olasunkanmi, M. M. Kabanda, S. Yesudass, I. Bahadur, A. S. Adekunle, I. B. Obot and E. E. Ebenso, *RSC Adv.*, 5 (2015) 76675.
9. R. Baskar, M. Gopiraman, D. Kesavan, K. Subramanian and S. Gopalakrishnan, *J. Mater. Eng. Perform.*, 24 (2015) 2847.
10. Y. Ren, Y. Luo, K. Zhang, G. Zhu and X. Tan, *Corros. Sci.*, 50 (2008) 3147.
11. S. Rajendran, S. P. Sridevi, N. Anthony, A. A. John and M. Sundearavadivelu, *Anti-Corros. Methods Mater.*, 52 (2005) 102.
12. N. A. Aljeaban, L. K. M. O. Goni, B. G. Alharbi, M. A. Jafar Mazumder, S. A. Ali, T. Chen, M. A. Quraishi, and H. A. Al-Muallem, *Int. J. Polym. Sci.*, Volume (2020) Article ID 9512680.
13. S. Kumar, H. Vashisht, L. O. Olasunkanmi, I. Bahadur, H. Verma, G. Singh, I. B. Obot and E. E. Ebenso, *Sci. Rep.*, 6(2016)30937
14. L. A. Al Juhaiman, *Int. J. Electrochem. Sci.*, 11 (2016) 2247.
15. M. G. Tsoeunyane, M. E. Makhatha and O. A. Arotiba, *Int. J. Corros.*, Volume (2019) Article ID 7406409.
16. E. Agustian, J. Jessica, P. Untoro and A. Sulaswatty, *J. Kim. Terap. Indones.*, 20 (2018) 57.
17. E. A. Soliman, M. R. Elkatory, A. I. Hashem and H. S. Ibrahim, *Fuel*, 211(2018) 535.
18. A. M. Al-Sabagh, S. H. El-Hamouly, T. T. Khidr, R. A. El-Ghazawy and Sh. A. Higazy, *J. Dispersion Sci. Technol.*, 34 (2013) 1585.
19. A. Kadhim, A. K. Al-Okbi, D. M. Jamil, A. Qussay, A. A. Al-Amiery, T. S. Gaaz, A. A. H. Kadhum, A. B. Mohamad, M. H. Nassir, *Results Phys.* 7 (2017) 4013.
20. M. A. Chidiebere, E. E. Oguzie, L. Liu, Y. P. Li and F. Wang, *Mater. Chem. Phys.*, 156 (2015) 95.
21. H. Ashassi-Sorkhabi, B. Shaabani and D. Seifzadeh, *Appl. Surf. Sci.*, 239 (2005) 15.
22. B. De Roover, M. Sclavons, V. Carlier, J. Devaux, R. Legras and A. Momtaz, *J. Polym. Sci., Part A: Polym. Chem.*, 33 (1995) 829.
23. R. Mani, M. Bhattacharya, J. Tang, *J. Polym. Sci. Part A: Polym. Chem.*, 37 (1999) 1693.
24. N. Soraya, D. j. Rayenne, M. Boulanouarc and O. Rabah, *Port. Electrochim. Acta.*, 36 (2018) 23.
25. W. Li, Z. Zhang, Y. Zhai, L. Ruan, W. Zhang and L. Wu, *Int. J. Electrochem. Sci.*, 15 (2020) 722.
26. Y. Elkhofsi, I. Forsal, E. M. Rakib and B. Mernari, *Port. Electrochim. Acta.*, 36 (2018) 77.
27. A. Fiala, W. Boukhedena, S. E. Lemallem, H. B. Ladouani, H. Allal, *J. Bio-Tribo-Corros.*, 5 (2019) 42.
28. H. Al-Sawaad, *J. Mater. Environ. Sci.*, 2 (2011) 128.
29. K. Zhang, W. Yang, X. Yin., Y. Chen., Y. Liu., J. Le. and B. Xu, *Carbohydr. Polym.*, 181 (2018) 191.
30. J. A. Bhat and V. Alva, *Indian J. Chem. Technol.*, 16 (2009) 228.
31. H. Z. Al-Sawaad, Z. N. Kadhim and M. A. Mahadi, *J. Chem. Pharm. Res.*, 11 (2020) 1386.
32. R. Solmaz, G. Kardaş, B. Yazıcı and M. Erbil, *Colloids Surf. A*, 312 (2008) 7.
33. M. H. Hussin and M. J. Kassim, *Mater. Chem. Phys.*, 125 (2011) 461.
34. A. S. Fouda, A. A. Al-Sarawy and E. E. El-Katori, *Desalination*, 201(2006)1.

35. H. Al-Sawaad., *Int. J. Electrochem. Sci.*, 8 (2013) 3105.
36. I. Ahmad and M. A. Quraishi, *Corros. Sci.*, 51(2009) 2006.
37. P. Singh and M. A. Quraishi, *Measurement*, 86 (2016) 114.
38. O. Benali, L. Larabi, B. Tabti and Y. Harek, *Anti-Corros. Methods Mater.*, 52 (2005) 280.
39. O. Benali, L. Larabi, S. M. Mekelleche. and Y. Harek, *J. Mater. Sci.*, 41 (2005) 7064.
40. J. D. Talati and D. K. Gandhi, *Corros. Sci.*, 23 (1983) 1315.
41. A. X. Stangu and U. Vijayalakshmi, *J. Asian Ceram. Soc.*, 6 (2018) 20.
42. M. Erna, H. Herdini and D. Futra, *Int. J. Chem. Eng.*, Volume (2019) Article ID 8514132.

© 2020 The Authors. Published by ESG ([www.electrochemsci.org](http://www.electrochemsci.org)). This article is an open access article distributed under the terms and conditions of the Creative Commons Attribution license (<http://creativecommons.org/licenses/by/4.0/>).